공학석사학위논문

고분자 계층 구조물의 전사 프린팅 공정을 통한 멀티스케일 금속 패턴 제작

Fabrication of multiscale metal patterns with polymeric hierarchical stamps by transfer printing method

2013 년 2 월

서울대학교 대학원

기계항공공학부

박 현 철

고분자 계층 구조물의 전사 프린팅 공정을 통한 멀티스케일 금속 패턴 제작

Fabrication of multiscale metal patterns with polymeric hierarchical stamps by transfer printing method

지도교수 서 갑 양

이 논문을 공학석사 학위논문으로 제출함

2013 년 2 월

서울대학교 대학원
기계항공공학부
박 현 철

박현철의 공학석사 학위논문을 인준함

2013 년 2 월

위 원 장 이 정 훈

부위원장 서 갑 양

위 원 전 누 리

Fabrication of multiscale metal patterns with polymeric hierarchical stamps by transfer printing method

Hyunchul Park

School of Mechanical and Aerospace Engineering

Seoul National University

Korea

Abstract

With the advances of micro/nano structures in the field of electronic, optical, fluidic and biomedical devices, there is a growing need to fabricate multiscale patterns and hierarchical structures in a simple and low-expertise manner. We present a simple method for transferring multiscale metal patterns on flat and patterned substrates by using hierarchical polymeric stamps made of UV-curable perfluoropolyether (PFPE). A dual-scale PFPE structure was made via two-step molding process under partial photocrosslinking conditions with a conversion ratio in the range of 35 to 45%. Micro- and nanoscale combined structures were generated over a large area (~10 cm^2) with high physical integrity with various length scales from 10 to 500-μm for the base microstructure and from 150 nm to 10-μm for the secondary structure. The hierarchical PFPE stamp enabled multiscale transfer printing (MTP) of metal pattern in single printing step on flat and patterned surfaces with recessed regions, which was impossible with a single-scale PFPE stamp.

Key Words : Hierarchical structure, transfer printing, multiscale metal pattern, molding

Student Number: **2011-22887**

Contents

List of Figures

Figure 4. SEM images of various transferred dual-scale metal patterns: (A) Au nanodot arrays (diameter: 150 nm, height: 30 nm) patched by 10-μm diameter circular patterns, nanoscale dots (300 nm diameter, Pt) (B) and lines (400 nm width, Al) (C) on the same base micropillars of 20 μm diameter. (D) Nanoscale dots (300 nm diameter, Au) formed in a discrete concentric pattern (see the hierarchical stamp shown in Figure 3D). (E) A nanoscale stencil (hole diameter: 250 nm) formed in the shape of 20 μm diameter circles. (F) Three-dimensional AFM image of (E) and (G) its cross-sectional profile between A and A' in (F).

Figure 5. (A) Schematic illustrations comparing the use of singe- and dual-scale stamps to transfer multiscale metal patterns on the recessed regions of the holey patterned substrate. (B) SEM images of the transferred Au patterns within 500-μm diameter microwells of 50-μm height.

Figure 6. Schematic illustrations of a stamp under a compressive stress and SEM images of MTP process with single- and dual-scale stamps. (A) Roof collapse occurs in the transferred metal array for a single-scale stamp and (B) no roof collapse occurs for a dual-scale stamp due to the enhanced height of the contact region.

Figure 7. Plot of the critical compressive stress as a function of spacing distance for single- and dual-scale stamps. Here, a simple line-and-space pattern was used for the bottom and upper structures: a line-and-space pattern (width = 150 nm, AR = 1, width/space = 1:1) for the upper structure and a line-and space pattern (width = 100 μm, AR = 1) for the bottom structure.

Nomenclature

v	Poisson's ratio
E	Young's modulus
σ_∞	Compressive stress
σ_c	Maximum compressive stress
γ	Surface energy
I	Absorption intensity
α	Conversion ratio
h	Height of line pattern
a	Width of line pattern
w	Spacing between the adjacent lines

1. Introduction

Stamp-based printing techniques, which involve direct transfer of functional materials to a target substrate, have been extensively studied over the past decades.[1-3] With the advances of new electronic, optical, fluidic and biomedical devices, there is a growing need to fabricate multiscale, hierarchical structures in a simple and low-expertise manner.[4-6] To date, diverse unconventional printing techniques have been developed such as microcontact printing (μCP),[7-8] detachment nanolithography,[9-11] decal transfer lithography,[12-13] and nanotransfer printing (nTP).[14-16] Of these, nTP has shown the ability to generate various metal arrays on a target substrate by utilizing an affinity (or adhesion) difference of a deposited metal film between a donor stamp (typically, polydimethylsiloxane, PDMS) and a receiving substrate. It was shown that the geometrical design and material property of the stamp play key roles in ensuring reliable metal transfer without stamp deformations such as buckling, lateral collapse, and roof collapse.

Until now, the stamp design in nTP has been in such a way that only single-scale structures were presented with the same height in the protruding parts of the stamps. In this case, there are some limitations for multiscale metal patterning having a relatively large gap between neighboring groups of patterns.[17-18] For example, if a designed pattern consists of groups of 100 nm dots separated by 1 to 10 μm spacing, a single-scale polymeric stamp hardly produces such a multiscale pattern in one-step printing since the space part would touch the substrate (roof collapse) while enforcing the stamp in conformal contact to the substrate. Furthermore, it would be hard to transfer patterns on recessed regions of a substrates (e.g., holey patterned substrate) with a single-scale stamp. It is noted in this regard that many electronic and microfluidic devices require a non-flat

or curved substrate as well as multiscale patterns with various length scales. Traditionally, a relatively complicated process involving a series of photolithography and selective etching has been used in order to achieve a metal pattern with multiple length scales on target substates.[19-20]

Here, we present a one-step, multiscale transfer printing (MTP) method using a monolithic hierarchical stamp of perfluoropolyether (PFPE) to fabricate dual-scale metal patterns on flat and patterned substrates. A key idea is to utilize an inert polymeric stamp of PFPE with hierarchical structures in the form of nanoscale pillars or lines that are monolithically integrated with microstructural bases. The microstructural base allows for a sufficient structural height to ensure a robust, conformal contact to the substrate. Such a hierarchically organized architecture is similar to the gecko's toe pad, which is known to enhance structural compliance and thus induces conformal contact via contact splitting.[21-22] In addition, multiscale metal patterns were transferred even within the recessed regions of the substrate owing to an enhanced structural height of nanoscale structures.

2. Results and Discussion

In our previous works, we demonstrated that dual-scale structures could be fabricated via two-step capillary force lithography (CFL)[23] or vacuum-assisted CFL[24] with a UV-curable material (e.g., polyurethane acrylate, PUA) by employing partial curing kinetics in the presence of oxygen environment. In this study, a UV-curable PFPE, which has low surface energy and high permeability, is used to form a monolithic hierarchical structure for efficient transfer printing process. There are several notable advantages in using the PFPE as a stamp material. First, the PFPE has a relatively high permeability[25-26] allowing for a large process window in the partially-cured regime. Second, it has low surface energy of 15.8 mJ m^{-2}; the metal layer can be easily transferred to the underlying substrate without additional surface modifications.[27-28] Third, it is mechanically stable (Young's modulus ~ 10.5 MPa) to maintain sub-100-nm structures without any structural collapse.[29]

Figure 1 depicts a schematic illustration for the fabrication process of multiscale metal pattern on flat/non-flat substrates using a UV-curable PFPE stamp with hierarchical structure. In the first molding step (first column in Figure 1), the PFPE resin was drop-dispensed on a flexible poly(ethylene terephthalate) (PET) film or silicon substrate. Then, the prepolymer spontaneously moves into the cavity by capillary action, and subsequently, the PFPE resin was incompletely cured utilizing the oxygen inhibition effect, resulting in a less-cured top layer on the fully-cured base structure. It is known that the oxygen acts as a scavenger against the initiator or free radicals, so that the surface remains tacky and partially-cured after photopolymerization.[30-31] After generating a base microstructure with partially-cured upper layer, nanoscale structures were monolithically integrated in the second molding step by placing a nanopatterned PUA mold in a vacuum (second

column in Figure 1). Using the two-step molding and partial curing presented here, micro- and nanoscale combined structures were generated with various length scales: from 10 to 500 μm for the base microstructure and from 150 nm to 10 μm for the secondary structure.

After preparing such a hierarchical PFPE stamp, a thin metal layer (e.g., Au, Al, Pt) was deposited to the thickness of 20~50 nm. For the MTP, the metal-coated hierarchical PFPE stamp was placed on flat and patterned receiving substrates (e.g., NOA73-coated Pyrex wafer, NOA: Norland Optical Adhesive), resulting in a selective pattern transfer via the difference of work of adhesion (third column in Figure 1). For flat surfaces, a roller was slightly rounded several times on the PFPE stamp to avoid an air trap as well as to induce conformal contact. For patterned surfaces, an alignment process was needed to locate the secondary structure within the recessed regions. With a manual alignment under an optical microscope with the aid of slight pressure, the multiscale metal patterns were faithfully formed selectively in the bottom of the microwell patterns.

To obtain a well-defined hierarchical structure of PFPE, care should be taken to adjust the degree of photocrosslinking of the base microstructures, for which the structural evolution of a partially-cured layer needs to be monitored with UV exposure time. For this purpose, Fourier transform infrared spectroscopy (FT-IR) analysis was performed as a function of UV exposure time up to 2 hr. (Figure 2A) Here, several peaks were identified as fingerprints of photopolymerization: C=O group located at 1720 cm^{-1}, C=C double bonds at 1530 cm^{-1}. As shown, these peaks were all decreased with the increase of exposure time and unchanged approximately after 120 sec. By comparing the relative

magnitude of these peaks, one can calculate the conversion ratio of each curing state, which can be used as an index to determine the photocrosslinking degree of the surface layer. Here, we used the C=C double bonds at 1530 cm^{-1} as a characteristic peak to calculate the conversion ratio as shown in Figure 2B.

In our experiment, the degree of polymerization in the partially-cured layer was controlled by UV exposure time in the first molding process. As shown in Figure 2C(i)-(iii), there are three distinct regimes for the photocrosslinked PFPE layer: cured, partially-cured, and uncured. In the partially-cured regime, the conversion ratio of the layer ranged between 35 and 45%, which gave rise to a well-defined hierarchical structure as shown in Figure 2C(ii). When the conversion ratio was higher (too rigid) or lower (too viscous) than this range, the hierarchical structure was either not formed (Figure 2C(i)) or collapsed (Figure 2C(iii)), respetively. It can be seen from the inset images that the base micro pillars were gradually flattened with lowering the exposure time, accompanying an increase of diameter from ~46 (completely cured) to ~48 (partially-cured) and ~60 μm (uncured), respectively. This suggests the importance of controlling the UV exposure time (30~60 s in this case) precisely in order to attain a suitably tacky layer. By controlling the degree of curing on the top surface of the base microstructure, physically well-integrated hierarchical structures were formed over a large area up to 10 cm^2.

Figure 4 displays SEM images of various multiscale metallic patterns (Au, Pt, and Al) formed by hierarchical PFPE stamps. Figure 4A shows 150-nm Au nanodot arrays (h = 30 nm) by the MTP process with the hierarchical PFPE stamps with 150-nm pillar arrays on the circular base microstructure of 10 μm diameter in Figure 3A. In total,

approximately 10^5 Au nanodots were transferred, with each 10 μm circular patch containing ~500 nanodots. In Figure 4B-C, groups of dots (300 nm diameter, Pt) and lines (400 nm width, Al) were formed in one-step transfer with a constant distance of 20 μm between the adjacent groups. This result demonstrates the ability to use different nanopatterns on the same microstructural bases. Similarly, groups of the same Au dots were formed in a discrete concentric pattern, which is the same hierarchical stamp shown in Figure 3D. Here, the thickness of metal layer was kept constant at ~40 nm. Furthermore, a nanoscale stencil (hole diameter: 250 nm) was faithfully transferred to the substrate in the shape of 20-μm diameter circles with the thickness of 40 nm (Figure 4E), as measured from the cross-sectional AFM measurement shown in Figure 4F-G.

The operating principle for the MTP process lies in the difference of work of adhesion at the metal-stamp and metal-substrate interfaces. The works of adhesion were calculated from the surface energy of each material in Table 1. The calculated works of adhesion were 54.02 and 99.01 mJ/m^2 for the Pt/PFPE and Pt/NOA73 as shown in Table 2, respectively, suggesting that the Pt layer could be readily transferred to the NOA73-coated substrate without any surface modification. Other metal layers like Au and Al rendered similar results so that the transfer will occur towards the receiving substrate.

Figure 5 highlights immediate advantages of using a hierarchical stamp when fabricating multiscale metal patterns in the recessed region of a holey patterned substrate. As shown, transferring such a multiscale pattern into hollow regions, which would be extremely difficult by conventional patterning methods with photolithography and deposition/etching, can be readily made with a dual-scale stamp. This is because the base

microstructure is mechanically robust and ensures a sufficient structural height to reach the bottom of the recessed region. In contrast, it would be hard to achieve this metal transfer with a single-scale stamp because the nanostructures have to be sufficiently high to touch the bottom substrate, which in turn results in a structural failure such as lateral collapse or self-mating (see the schematic in Figure 5A). A simple theoretical model is considered shortly to explain these contrasting behaviours with single- and dual-scale stamps. These results suggest that a hierarchical polymeric stamp offers a new route to transferring metal patterns selectively within hollow regions of the substrate, which would be particularly useful for many applications including physical modification of microfluidics, selective metal patterning for optical devices and sensors.

Here we elaborate on advantages and theoretical basis for the use of hierarchical PFPE stamps. Figure 6 shows direct comparisons between single- and dual-scale stamps when transferring groups of 20-μm Au dots (9 dots per each patch) that are separated by 100 μm. The two stamps have the same geometry except that the secondary structure is formed and equally separated by the base microstructure for the dual-scale stamp. As shown, there was a distinct difference in the resulting pattern transfer: roof collapse occurred for the single-scale stamp, such that the metal layer in the background was completely transferred to the substrate, as evidenced by the bright color in the background. This result reveals that roof collapse frequently occurs in multiscale metal patterns having a relatively large gap between neighboring features. In sharp contrast, no roof collapse was observed for the dual-scale stamp as seen from the black background under a same stress condition (σ_∞ = ~200 kPa), clearly demonstrating that the roof collapse is avoidable for a dual-scale stamp even when the distance between adjacent

features is larger than a critical value. In addition to the roof collapse, other structural defects like buckling and lateral collapse could be significantly reduced with hierarchical stamp geometry.

A simple theory can be used to explain the observed behaviors in terms of the critical aspect ratio (AR) without roof collapse. The maximum AR for a given stamp can be determined from an analysis of structural stability for repeating lines, which is given by[32]

$$\frac{-8\sigma_{\infty} w}{\pi E^{*} h}\left(1+\frac{a}{w}\right)\cosh^{-1}\left[\sec\left(\frac{w\pi}{2(w+a)}\right)\right]<1$$

where $E^{*}=E/(1-\nu^{2})\approx 4E/3$ (ν is the Poisson's ratio of the stamp material), h and a are the height and the width of lines, respectively, w is the spacing between the adjacent lines E is the Young's modulus of the material, and σ_{∞} is the compressive stress. A simple algebraic manipulation yields the following relation:

$$\sigma_{c}=\frac{-\pi E^{*} h}{8w\left(1+\frac{a}{w}\right)\cosh^{-1}\left[\sec\left(\frac{w\pi}{2(w+a)}\right)\right]}$$

where the critical stress (σ_{c}) is the maximum compressive stress that can be applied on the stamp without the formation of roof collapse. Obviously, if the distance between the adjacent lines is relatively large, the contact is prone to roof collapse as shown in Figure 6A. Here, the enhanced stability of hierarchical structure can be attributed to two aspects. First, the base microstructure provides an enough gap between the roof and the substrate,

thereby negating a possible touch of the roof. Second, the height of nanostructures needed to make conformal contact can be reduced significantly, which is responsible for strong resistance against lateral collapse as shown in Figure 5A. Shown in Figure 7 is a plot of σ_c as a function of space for single- and dual-scale stamps. For this plot, we assumed a line-and-space pattern for the secondary nanostructure (width = 150 nm, AR = 1, width/space = 1:1). It is clear from the figure that the dual-scale stamp is much stable than the single-scale stamp in the entire domain.

3. Conclusion

We have presented a simple method for multiscale metal transfer utilizing the two-step molding process with partial curing kinetics and enhanced mechanical stability of a dual-scale polymeric stamp. It turned out that a partially-cured layer of PFPE with a conversion ratio between 35 and 45% yielded highly integrated, monolithic hierarchical structures via the two-step molding process. Using these hierarhical structures and metal deposition, the MTP process was carried out in a single transfer onto flat and patterned substrates with recessed regions without notable mechanical deformations such as buckling, lateral collapse, and roof collapse. The current method would be useful in patterning multiscale metal arrays on flat and patterned substrates with potential applications to nano-optics, electric devices and sensors.

Experimental Section

***Preparation of PDMS and PUA molds**:*

PDMS molds were fabricated by the standard protocol (curing agent = 10 wt%, Sylgard 184 silicon elastomer, Dow Corning) on silicon masters. Similarly, the PUA molds were prepared following the procedure reported earlier.[33] The masters used in the base structure had dimensions from 5 to 500 μm in feature size with negative impressions. The masters for the upper structure had dimensions from 150 nm to 10 μm. For controlling the oxygen penetration depth, the thickness of PDMS mold was maintained approximately at 1 mm throughout the experiment.

Generation of polymeric hierarchical stamps of PFPE:

The PFPE-urethane methacrylate (MD700, Solvay Solexis, Italy) with a molecular weight of 1,500 was used as the prepolymer. Darocur 1173 (2-Hydro-2-methyl-1-1phenyl-1-propane) from Ciba Specialty Chemicals (Switzerland) was added as a photoinitiator to the mixture at 5.0 wt% with respect to the total amount of the blend of the prepolymer and reactive monomer diluents. Then, the mixture was thoroughly mixed prior to curing. In the first molding and UV curing process, the PFPE resin was drop-dispensed on a flexible PET film (50 μm thickness) or silicon substrate. Then, the PFPE resin was incompletely cured by UV exposure for 30~40 sec (λ = 250~400 nm, dose = 100 mJ/cm^2) at ambient conditions. After generating a base microstructure with partially-cured upper layer, a secondary structure was monolithically integrated in the second molding step by

placing a nanopatterned PUA mold with sufficient UV exposure for 3 min under a slight pressure (~200 kPa) in a vacuum.

***MTP process**:*

A thin metal layer (Au, Al, and Pt) was deposited on the fabricated hierarchical stamp using a thermal evaporator at a speed of 2 Å/s to the thickness of 20~50 nm. For the MTP process, Noland Optical Adhesive 73 (NOA73) was spin coated on a Pyrex wafer or a PET film as the receiving substrate. The metal-coated PFPE stamp was brought in contact with the substrate, and a roller was slightly rounded several times to avoid air traps as well as to induce uniform contact.

Scanning electron microscopy (SEM):

High-resolution SEM images were obtained using a JSM-7500F microscope (JEOL, Japan) operating at an accelerating voltage of 5~15 kV. To avoid charging effects, samples were sputter-coated with Pt and Au to the thickness of 10 nm prior to measurements.

Atomic forced microscopy (AFM):

AFM images were obtained using a XE-150 (Park Systems, Korea). The samples were imaged with tapping mode at ambient conditions. Some images were flattened and used without further manipulations.

Fourier transform infrared spectroscopy (FTIR):

The FTIR spectra were obtained using Vertex 70 with FT-IR spectrometer (BRUCKER). IR radiation was detected by a liquid-nitrogen-cooled mercury cadmium telluride detector. FT-IR data were obtained to monitor the degree of photopolymerization of PFPE as a function of UV exposure time. The conversion ratio was calculated by

$$\alpha(\%) = \frac{[I_{1530}]_0 - [I_{1530}]_t}{[I_{1530}]_0} \times 100$$

where $[I_{1530}]_0$ and $[I_{1530}]_t$ are the intensities of time = 0 (initial intensity) and t, respectively, for the C=C double bonds.

Contact angle measurement:

The probing liquids were de-ionized (DI) water for the polar component and formamide (de-ionized 99.5%, Sigma) for the dispersive component. The wetting angle measurement was performed on five different locations of flat solid surfaces using a Rame-Hart goniometer (Rame-Hart Inc., USA) at ambient conditions.

Table and Figures

Table 1. Measurement of surface energy with polar and dispersive terms

Material	Surface energy (mJ/m^2)		
	Polar	Dispersive	Total
NOA73	10.4	42.1	52.5
PFPE	4.3	11.5	15.8
Pt	12.9	34.6	47.5

Table 2. Works of adhesion between Pt/NOA73 and Pt/PFPE.

Interface	Work of adhesion (mJ/m^2)
Pt/PFPE	54.0
Pt/NOA73	99.0

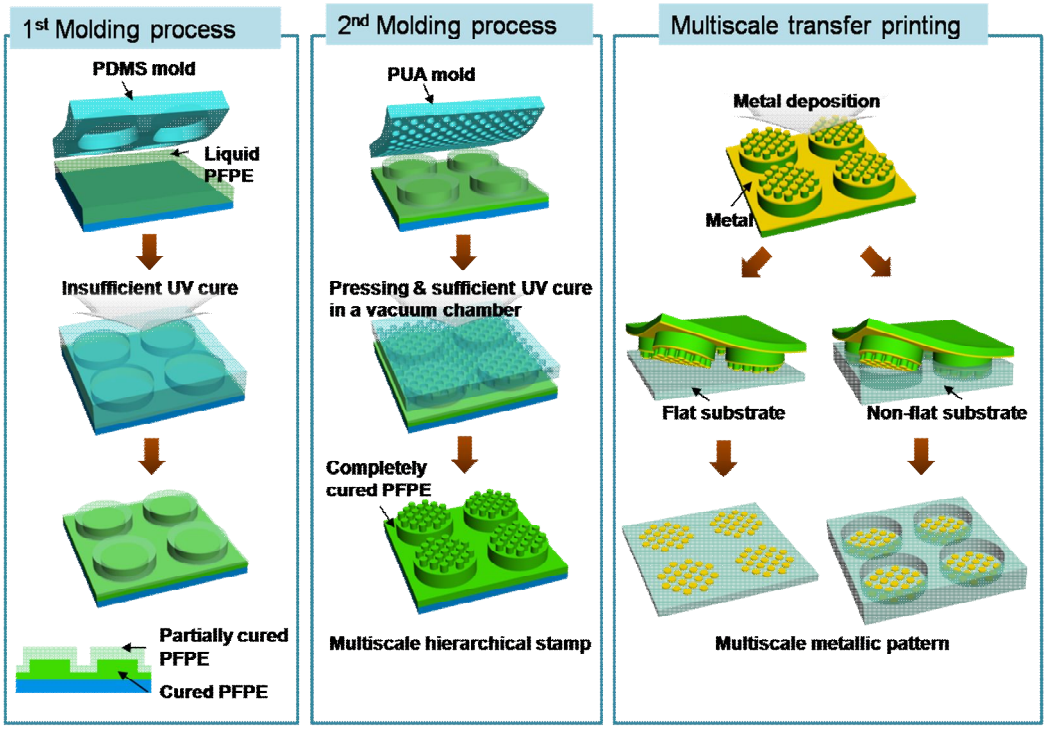

Figure 1. Two-step molding process for fabricating monolithic, hierarchical PFPE stamps and Multiscale transfer printing process to generate multiscale metal patterns on the flat/non-flat substrate using the highly controlled hierarchical PFPE stamps.

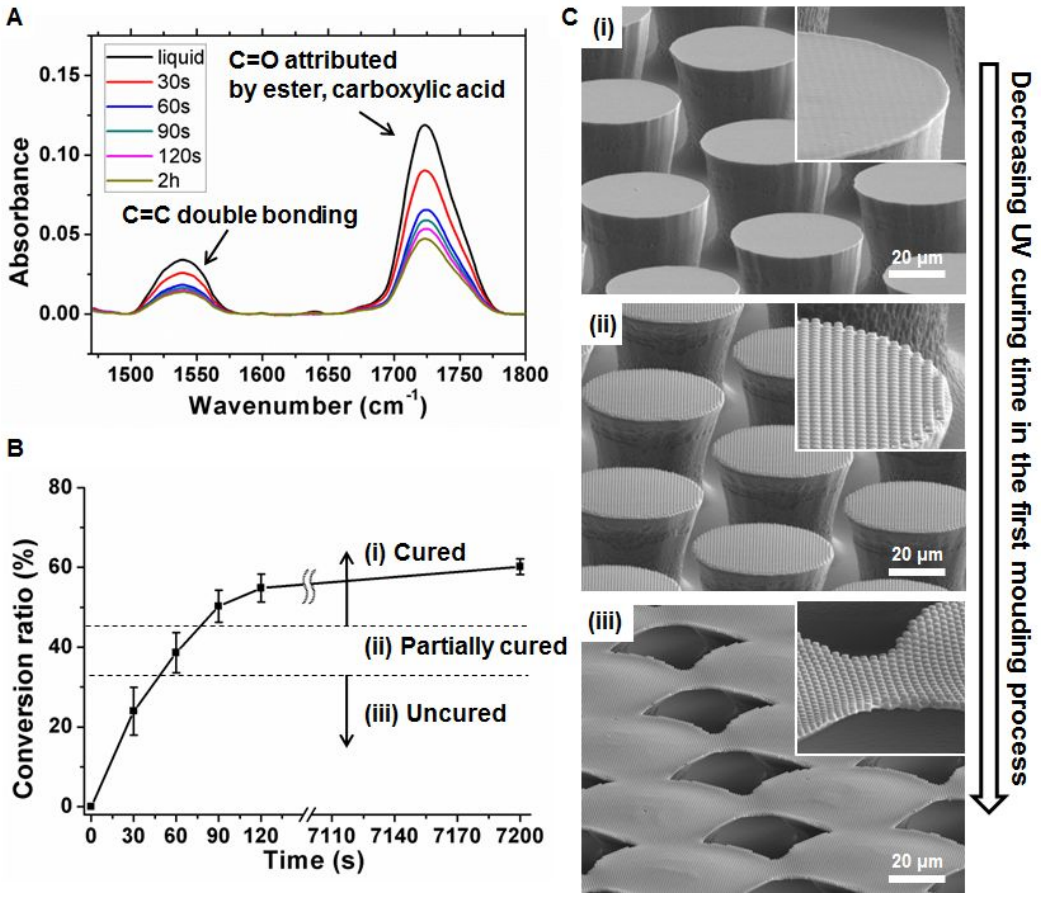

Figure 2. FT-IR analysis and SEM images of hierarchical structure depending on the UV exposure time in the first molding process. (A) FT-IR spectra showing the absorbance changes of C=O bonds at 1720 cm^{-1} and C=C bonds at 1530 cm^{-1} as a function of exposure time. (B) Change of the conversion ratio as a function of exposure time at 1530 cm^{-1}. As shown, three distinct curing regimes were identified: cured, partially-cured, and uncured regimes. (C) Representative hierarchical structures for each regime are shown: (i) cured, (ii) partially cured, and (iii) uncured regimes.

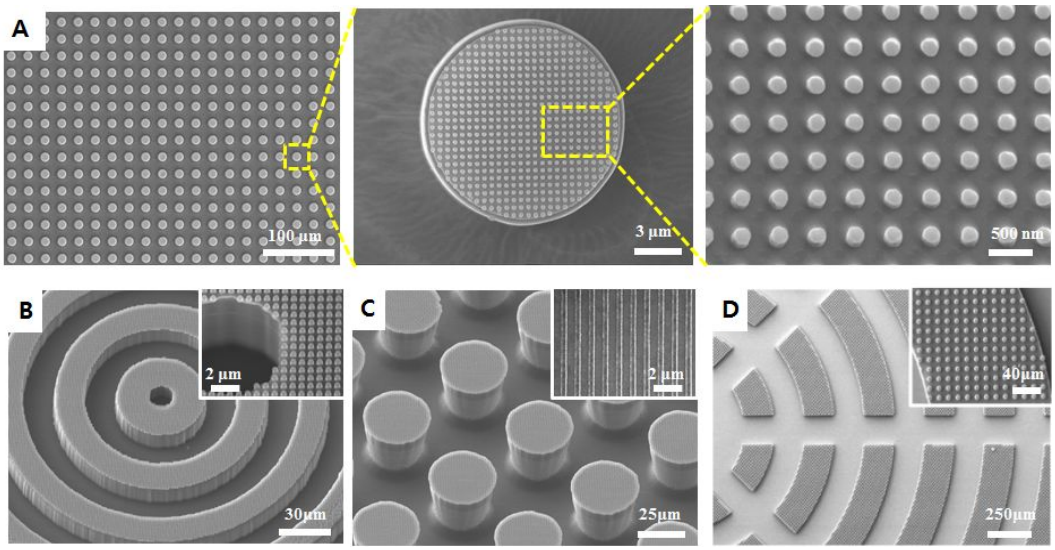

Figure 3. SEM images showing several monolithic hierarchical structures with various shapes and scales: (A) pillars (diameter: 150 nm, height: 150 nm) on cylinders (diameter: 10 μm, height: 10 μm), (B) 800-nm wide dots (width/space = 1:1, height: 800 nm) on concentric circles of 20 μm width, (C) 400 nm wide lines (width/space = 2:3) on pillars (diameter: 30 μm, height: 30 μm), and (D) 8-μm pillars on discrete concentric circles of 250 μm width.

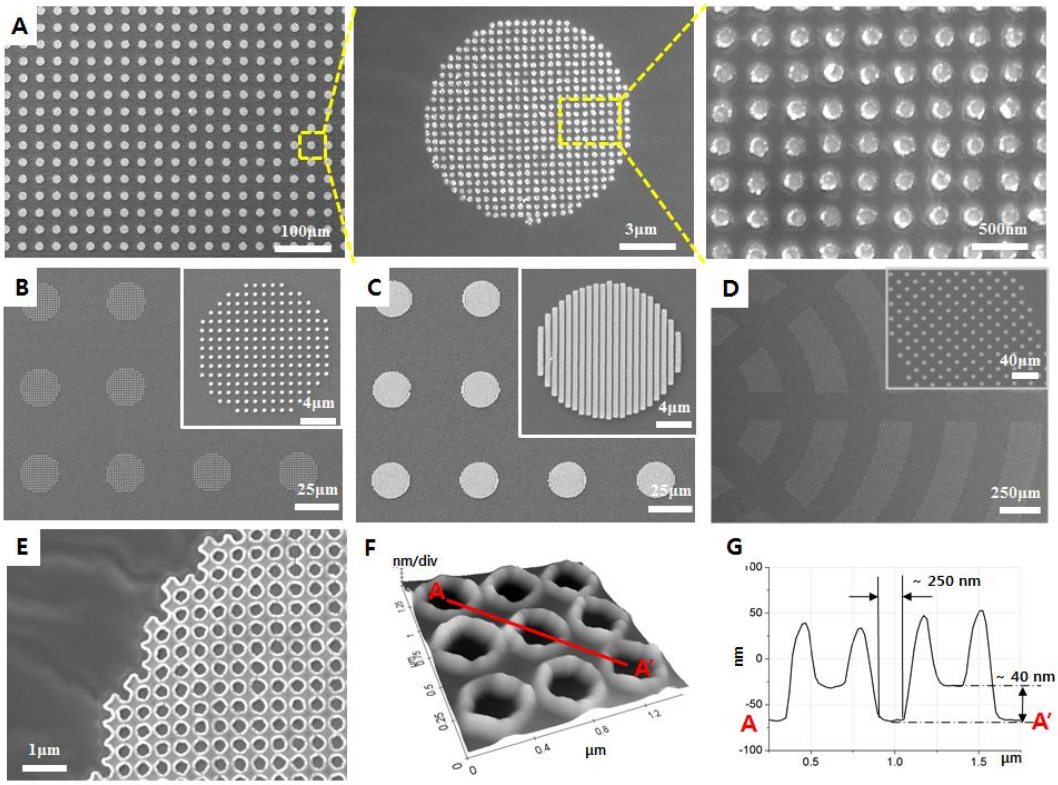

Figure 4. SEM images of various transferred dual-scale metal patterns: (A) Au nanodot arrays (diameter: 150 nm, height: 30 nm) patched by 10-μm diameter circular patterns, nanoscale dots (300 nm diameter, Pt) (B) and lines (400 nm width, Al) (C) on the same base micropillars of 20 μm diameter. (D) Nanoscale dots (300 nm diameter, Au) formed in a discrete concentric pattern (see the hierarchical stamp shown in Figure 3D). (E) A nanoscale stencil (hole diameter: 250 nm) formed in the shape of 20 μm diameter circles. (F) Three-dimensional AFM image of (E) and (G) its cross-sectional profile between A and A' in (F).

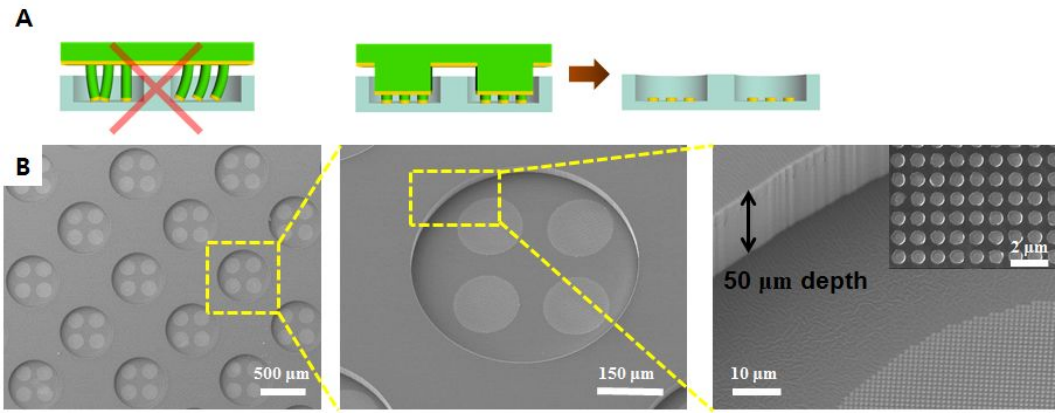

Figure 5. (A) Schematic illustrations comparing the use of singe- and dual-scale stamps to transfer multiscale metal patterns on the recessed regions of the holey patterned substrate. (B) SEM images of the transferred Au patterns within 500-μm diameter microwells of 50-μm height.

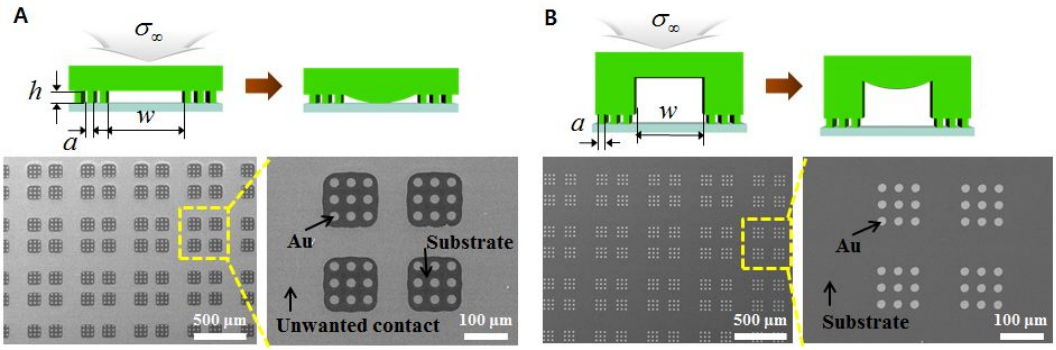

Figure 6. Schematic illustrations of a stamp under a compressive stress and SEM images of MTP process with single- and dual-scale stamps. (A) Roof collapse occurs in the transferred metal array for a single-scale stamp and (B) no roof collapse occurs for a dual-scale stamp due to the enhanced height of the contact region.

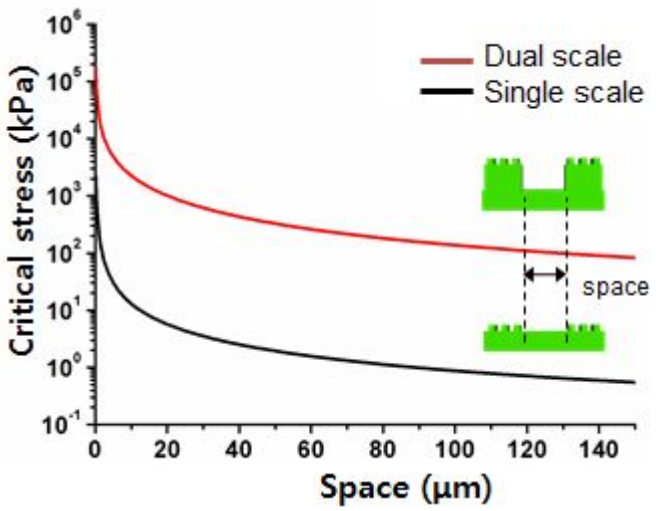

Figure 7. Plot of the critical compressive stress as a function of spacing distance for single- and dual-scale stamps. Here, a simple line-and-space pattern was used for the bottom and upper structures: a line-and-space pattern (width = 150 nm, AR = 1, width/space = 1:1) for the upper structure and a line-and space pattern (width = 100 μm, AR = 1) for the bottom structure.

References

[1] A. Carlson, A. M. Bowen, Y. G. Huang, R. G. Nuzzo, J. A. Rogers, *Adv Mater* **2012**, *24*, 5284.

[2] T. H. Kim, K. S. Cho, E. K. Lee, S. J. Lee, J. Chae, J. W. Kim, D. H. Kim, J. Y. Kwon, G. Amaratunga, S. Y. Lee, B. L. Choi, Y. Kuk, J. M. Kim, K. Kim, *Nat Photonics* **2011**, *5*, 176.

[3] B. H. Lee, Y. H. Cho, H. Lee, K. D. Lee, S. H. Kim, M. M. Sung, *Adv Mater* **2007**, *19*, 1714.

[4] X. F. Gao, X. Yao, L. Jiang, *Langmuir* **2007**, *23*, 4886.

[5] Y. Zhang, C. T. Lin, S. Yang, *Small* **2010**, *6*, 768.

[6] J. J. Chae, S. H. Lee, K. Y. Suh, *Adv Funct Mater* **2011**, *21*, 1147.

[7] J. Foley, H. Schmid, R. Stutz, E. Delamarche, *Langmuir* **2005**, *21*, 11296.

[8] D. Qin, Y. N. Xia, G. M. Whitesides, *Nat Protoc* **2010**, *5*, 491.

[9] J. K. Kim, K. Y. Suh, *Appl Phys Lett* **2008**, *92*, 22.

[10] M. K. Kwak, T. I. Kim, P. Kim, H. H. Lee, K. Y. Suh, *Small* **2009**, *5*, 928.

[11] S. H. Sung, H. Yoon, J. Lim, K. Char, *Small* **2012**, *8*, 826.

[12] W. R. Childs, R. G. Nuzzo, *Langmuir* **2005**, *21*, 195.

[13] P. Kim, R. Kwak, S. H. Lee, K. Y. Suh, *Adv Mater* **2010**, *22*, 2426.

[14] E. Menard, L. Bilhaut, J. Zaumseil, J. A. Rogers, *Langmuir* **2004**, *20*, 6871.

[15] T. I. Kim, J. H. Kim, S. J. Son, S. M. Seo, *Nanotechnology* **2008**, *19*, 295302.

[16] D. Chanda, K. Shigeta, S. Gupta, T. Cain, A. Carlson, A. Mihi, A. J. Baca, G. R. Bogart, P. Braun, J. A. Rogers, *Nat Nanotechnol* **2011**, *6*, 402.

[17] W. Zhou, Y. Huang, E. Menard, N. R. Aluru, J. A. Rogers, A. G. Alleyne, *Appl Phys Lett* **2005**, *87*, 251925.

[18] Y. G. Y. Huang, W. X. Zhou, K. J. Hsia, E. Menard, J. U. Park, J. A. Rogers, A. G. Alleyne, *Langmuir* **2005**, *21*, 8058.

[19] J. Henzie, M. H. Lee, T. W. Odom, *Nat Nanotechnol* **2007**, *2*, 549.

[20] D. Bhandari, I. I. Kravchenko, N. V. Lavrik, M. J. Sepaniak, *J Am Chem Soc* **2011**, *133*, 7722.

[21] A. del Campo, C. Greiner, E. Arzt, *Langmuir* **2007**, *23*, 10235.

[22] H. E. Jeong, K. Y. Suh, *Nano Today* **2009**, *4*, 335.

[23] H. E. Jeong, R. Kwak, J. K. Kim, K. Y. Suh, *Small* **2008**, *4*, 1913.

[24] R. Kwak, H. E. Jeong, K. Y. Suh, *Small* **2009**, *5*, 790.

[25] J. Scheirs, *Modern fluoropolymers : high performance polymers for diverse applications*, Wiley, Chichester ; New York, **1997**.

[26] S. S. Williams, S. Retterer, R. Lopez, R. Ruiz, E. T. Samulski, J. M. DeSimone, *Nano Lett* **2010**, *10*, 1421.

[27] T. T. Truong, R. S. Lin, S. Jeon, H. H. Lee, J. Maria, A. Gaur, F. Hua, I. Meinel, J. A. Rogers, *Langmuir* **2007**, *23*, 2898.

[28] J. R. Niskala, W. You, *J Am Chem Soc* **2009**, *131*, 13202.

[29] J. K. Kim, D. E. Lee, W. I. Lee, K. Y. Suh, *Nanotechnology* **2010**, *21*, 295306.

[30] H. E. Jeong, K. Y. Suh, *Lab Chip* **2008**, *8*, 1787.

[31] H. E. Jeong, J. K. Lee, H. N. Kim, S. H. Moon, K. Y. Suh, *P Natl Acad Sci USA* **2009**, *106*, 5639.

[32] C. Y. Hui, A. Jagota, Y. Y. Lin, E. J. Kramer, *Langmuir* **2002**, *18*, 1394.

[33] S. J. Choi, H. N. Kim, W. G. Bae, K. Y. Suh, *J Mater Chem* **2011**, *21*, 14325.

고분자 계층 구조물의 전사 프린팅 공정을 통한 멀티스케일 금속 패턴 제작

서울대학교 공과대학 대학원
기계항공공학부
박 현 철

요 약

스탬프 기반 프린팅 기법은 마이크로와 나노스케일 패턴을 쉽고 빠르게 형성할 수 있는 기술로 넓은 응용 영역에 걸쳐 활용되는 기술이다. 스탬프 기반의 프린팅 공정에서 미세한 패턴의 정확도를 결정하는 가장 중요한 요소는 스탬프의 강성과 형상이다. 기존에 사용되는 고분자 단일 스케일 스탬프의 경우는 단일 디멘젼의 패턴을 만들기에 적합하지만 나노와 마이크로 스케일이 복합적으로 혼합된 멀티스케일 패턴을 형성하려면 2 회 이상의 프린팅 작업이나 에칭, 리프트오프 등과 같은 복잡한 공정이 필요하다. 본 논문에서는 멀티스케일 패터닝을 위해 자외선 경화성 고분자의 기계적 강도를 정량적으로 조절하여 스탬핑에 최적화된 형상으로 고분자 계층 구조물을 제작하였다. 계층 구조체는 상단부 나노 구조물과 하단부 마이크로 구조물로 구성되는데, 하단부 마이크로 구조물이 충분한 강성과 높이를 제공하여 스탬프의 변형 없이 프린팅 공정이 가능하다. 결국, 제작된 계층 구조물을 스탬프로 사용하여 기존의 단일 구조물로 제작이 어려웠던 멀티스케일 금속 패턴을 손쉽게 구현하였다. 특히, 1 회의 전사 프린팅 공정으로 평탄한 기판뿐 아니라 마이크로 스케일의 패턴을 가진 기판의 바닥면까지 손쉽고 빠르게 멀티스케일 패턴을 형성할 수 있는 방법을 고안한 것에 의의가 있다.

주 요 어: 계층 구조, 전사 프린팅 공정, 멀티스케일 금속 패턴, 몰딩

학 번: 2011-22887